

Controlling Congestion via In-Network Content Adaptation

Yongzhou Chen, Ammar Tahir, Radhika Mittal

UIUC

Abstract

Realizing that it is inherently difficult to precisely match the sending rates at the endhost with the available capacity on dynamic cellular links, we build a system, Octopus, that sends real-time data streams over cellular networks using an imprecise controller (that errs on the side of over-estimating network capacity), and then drops appropriate packets in the cellular network buffers to match the actual capacity. We design parameterized primitives for implementing the packet dropping logic, that the applications at the endhost can configure differently to express different content adaptation policies. Octopus transport encodes the app-specified parameters in packet header fields, which the routers parse to execute the desired dropping behavior. Our evaluation shows how real-time applications involving standard and volumetric videos can be designed to exploit Octopus, and achieve 1.5-50 \times better performance than state-of-the-art schemes.

1 Introduction

Congestion control solutions predominantly rely on the endhost picking the right sending rate to match the network capacity that is estimated using network feedback. The feedback could be implicit (e.g. packet drops [35, 38] or delay [18, 20, 50, 69, 72]) or may involve more active involvement from the routers (e.g. early congestion notifications [10, 29, 33, 65, 76], early drops [2, 30], and explicit rate signalling [45, 64]). We collectively refer to such schemes as feedback-based controllers.

It is important for a feedback-based controller to precisely match the sending rate with network capacity – sending too little leads to low throughput, and sending too much leads to high queuing delays and packet drops. Inter-flow scheduling schemes (e.g. fair queuing or flow prioritization [11, 23, 54, 57, 60, 61]) can provide isolation across flows, but minimizing the self-inflicted queuing delay for a given flow still relies on precise feedback-based congestion control. However, as we show in §2, it is not possible to precisely control sending rate using a feedback-based controller when network capacity changes at timescales that are smaller than the time taken to get feedback from the network (as is common in case of dynamic cellular links [33, 51, 52, 55, 69]).

In this paper, we explore an alternative approach that sidesteps the need for a precise feedback-based controller: we allow

the sender to send too much to ensure high throughput, and then adapt the transmitted content in network buffers by semantically dropping packets to match the available capacity and minimize delay.

As a motivating usecase, we consider real-time data streams sent over cellular downlinks (e.g. for video conferencing, virtual reality, etc).¹ Real-time streams, comprising of a series of multi-packet *messages* (e.g. video frames), can typically adapt their content (e.g. video frame rate or quality) based on available network capacity in order to achieve low message latency. The state-of-the-art real-time transmission schemes (primarily focusing on real-time video, e.g. [21, 31, 40, 73]) use a feedback-based controller to estimate network bandwidth, with the application then adapting its content based on this estimate. However, given the inherent difficulty in accurately estimating the dynamic cellular link capacity, the feedback-based controllers either underestimate it [2, 69] (leading to low throughput and content quality), or overestimate it [20, 35] (leading to high lag in message delivery).

We propose sending real-time streams using an imprecise feedback-based controller (that errs on the side of overestimating network bandwidth) and then adapting the transmitted content by dropping “appropriate” packets in the cellular router buffers. We build a system, Octopus, to enable such in-network content adaptation.

So how do we go about doing in-network content adaptation? First of all, it requires the real-time application (app) to encode its streams in a way that supports content adaptation via packet drops. As detailed in our case-studies (§6), existing stream encoding techniques (e.g. scalable video codec [6, 59, 67] and point clouds for volumetric videos [37, 48]) already provide such adaptability. The in-network packet dropping logic would then depend on the app’s requirements and how it encodes the stream. For instance, some streams may support reducing the spatial resolution (e.g. by dropping packets corresponding to higher quality layers in a layered video stream [6, 59], or to higher density levels in a point cloud [37]), whereas others may solely allow reducing temporal resolution (e.g. by dropping certain frames).

This leads us to the following question: how do we support different packet dropping policies that may vary across applications? Since it is not practical for cellular routers to

¹We focus on scenarios where the cellular downlink is the bottleneck; we can handle uplink bottlenecks by similar content adaptation at the end-device.

implement customized dropping logic specific to each app, we look for generalized dropping *primitives* which can be configured differently by different apps to express their requirements. The mode of configuration we adopt involves parameters that can be specified in packet header fields.

We first considered using well-known queue management techniques for this that seemingly provide such configurability. One option was to use priority dropping [5, 15], where the app marks different packets with different priorities, and the router drops lower priority packets when the buffer is full. Another option was to tag different packets with deadlines, and the router drops the packets that exceed their deadline [68]. However, it was not immediately obvious how an app could use these schemes to express their content adaptation policies that often involve complex dependencies across frames. For instance, if the app requires minimizing the latency of the latest message, how do we tune the buffer threshold for priority dropping or the packet deadlines, the optimal value for which would vary with message sizes and network bandwidth.

So we instead design parameterized dropping primitives to more directly capture the requirements of real-time apps. Our primitives drop packets at the granularity of multi-packet messages, where the app specifies the message boundaries, and expresses its dropping policy as per-message parameters. Our primitive trigger message drops based on two natural conditions: (1) arrival of a new message, where the app can specify which messages trigger a drop in which subset of older queued-up messages using priority levels, and (2) when the link capacity falls below specified bitrate thresholds, where the app can configure different thresholds for different messages based on the (known) bitrate of the generated content. Apps can configure these primitives by setting message parameters to express different content adaptation policies, in a manner that is agnostic of underlying network characteristics.

Centered on the above primitives, we build a system, Octopus, that comprises of: (i) an interface for applications to specify their message boundaries and per-message parameters to configure the dropping primitives (ii) a transport protocol that encodes the app-specified message parameters into packet headers, performs (imperfect) congestion control, and implements the parameterized dropping primitives for content adaptation in transport buffer, (iii) router buffer management scheme that implements the dropping primitives, and parses the parameters in packet header fields to enforce app-specified content adaptation policy.

We acknowledge that our system cannot be *immediately* deployed, as it requires changes at both the endpoints and the cellular base-stations. However, we believe that our approach presents an interesting design point that is worth exploring, given the increasing volume and significance of real-time streaming [8, 36] that is well-suited to in-network content

adaptation, the increasing flexibility of modern network infrastructure [16, 17, 71], and the scope for significant improvement in performance (as promised by our evaluation).

We summarize our key contributions below:

- We present a new approach for controlling congestion that is based on adapting the transmitted content inside the network, rather than trying to perfectly match the sending rate with estimated network capacity at the endhost.
- We design a system to realize this new approach (§4), which is centered around parameterized primitives that can be used to express different content adaptation policies.
- We prototype our system (§5) using UDT [34] (a user-space transport framework) for the endhost logic, and srsRAN [32] (an open-source cellular platform) for the in-network logic.
- We evaluate our prototype using three different case-studies (§6), and across a variety of scenarios (§7), to show how our approach results in 1.5-50× better performance than state-of-the-art schemes [31, 37, 73].

2 Motivation

The cellular link from the base-station to the user device is often the bottleneck for data transmission [12, 69, 74]. These links are prone to bandwidth (capacity) variations [33, 69, 72], triggered by dynamic obstacles or changing directionality or distance as a device moves. We conducted a series of experiments to evaluate how well a feedback-based congestion controller performs on a volatile cellular network. We used Mahimahi [53] to emulate a link with 60ms base round-trip time (RTT), 375KB buffer size, and time-varying bandwidth drawn from a Verizon trace [53]. A sender attached to the emulated link sends backlogged data to a receiver, using different congestion controllers.

Prior works fail to achieve both high link-utilization and low queuing. Figure 1(a) shows that TCP BBR[20] (designed for WAN) achieves high link utilization, but also results in high queuing delays, that reach up to 500 milliseconds. We see similar results with TCP Cubic (not shown for brevity). This led to development of congestion controllers for cellular networks that react faster to changing network bandwidth [33, 69, 72]. Our experiment with Sprout [69] revealed how it can be too cautious resulting under-utilization of link capacity, and even then it cannot avoid spikes in delay when bandwidth suddenly plunges (Figure 1(b)). Schemes that use a feedback-based congestion controller with AQM, such as Cubic+Codel and ABC[33], show similar issues of under-utilization and delay spikes (Figure 1(c,d)).

We cannot practically design a perfect congestion controller! The above were but a few samples from the vast repertoire of congestion control algorithms designed for wide-area and cellular networks [20, 25, 26, 33, 35, 69, 70, 72].

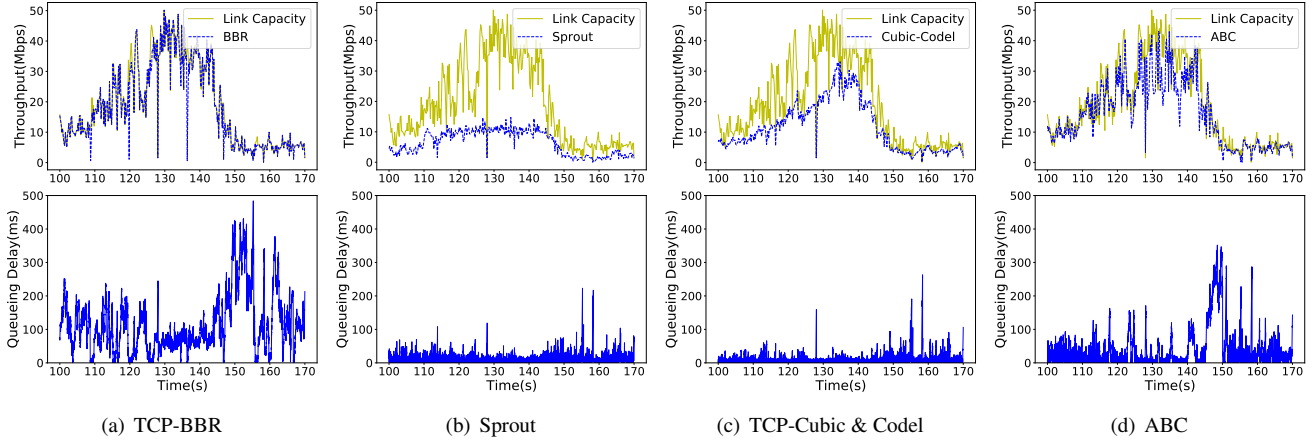


Figure 1: Throughput (top) and queuing delay (bottom) for different protocols on a link emulating Verizon download trace with RTT 60ms. We cut-off the delay graphs at 500ms to better highlight queuing over time.

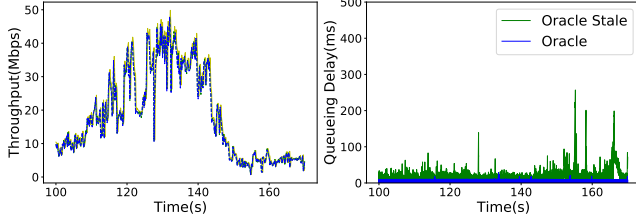


Figure 2: Throughput and queuing delay for Oracle on a link emulating Verizon download trace with RTT 60ms.

This raises the natural question of whether a different controller would have perfectly achieved high link utilization and consistently low queuing delay? Rather than taking up the insurmountable task of experimenting with all proposed congestion controllers, we instead exploited our emulation environment to do a simple exercise. We implemented an “Oracle” that used the knowledge of the emulated bandwidth trace to compute the number of packets that the link can serve over each period of 5ms, and sent precisely those many packets during that time period. We observed that this indeed resulted in perfect behavior (maximal link utilization with queuing delay consistently below 30ms).

We then added a small offset, making the sending rate stale by 5ms compared to the link capacity. This staleness models real-world scenarios where an endhost can receive network feedback only after some inevitable delay.

Figure 2 shows the resulting performance. We find that even with an offset as small as 5ms, our Oracle was unable to avoid spikes in queuing. The queue keeps accumulating packets that arrive 5ms late during a bandwidth reduction (thus missing their chance to be transmitted), until the next increase in bandwidth allows transmitting them.

These results show that spikes in queuing delay cannot be avoided without knowledge of (i) precisely how long a packet would take to reach the base-station, and (ii) the available

bandwidth at that (future) time which may change based on external factors such as a sudden obstacles. Since it is not possible to obtain such information in practice, we do not expect any feedback-based congestion controller to behave perfectly.

Our approach. Given the pessimistic results above, how can we meet the stringent throughput and latency requirements of networked real-time apps? Our system, Octopus, side-steps the problem of designing a perfect feedback-based congestion controller by using a reactive approach that exploits the content adaptability of real-time streams. Octopus sends data using BBR congestion control to achieve high link utilization, and then drops appropriate packets in the cellular network buffers to match the actual available link capacity and minimize queuing delay. We design parameterized primitives for implementing the dropping logic, that the applications at the endhost can configure differently to express different content adaptation policies. Octopus transport encodes the app-specified parameters in packet header fields, which the routers can parse to execute the desired dropping behavior. We provide a detailed description of Octopus’ design in §4.

3 Related work

Packet scheduling. Scheduling packets *across* different flows (e.g. to achieve fairness or small flow completion time) [11, 23, 54, 57, 60, 61] is orthogonal and complementary to our goals of ensuring optimal throughput and latency for a given real-time flow. In the context of intra-flow scheduling, recent work [13, 44] analyze the benefits of using LCFS (last-come-first-serve) for maximizing freshness at per-packet granularity. Since a real-time message is typically consumed by the receiver as soon as it is received, there is little value to delivering an older message out-of-order, after a later message in the stream has been delivered. Therefore, rather than determining the packet scheduling order, the key question we consider

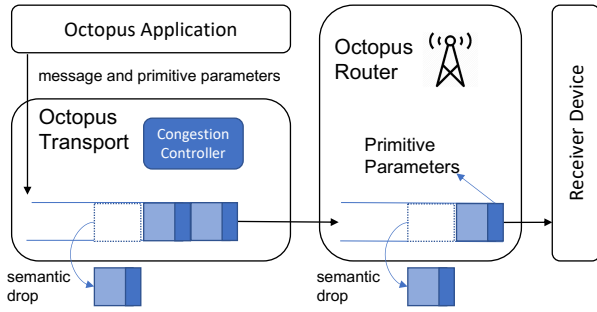


Figure 3: Octopus Framework Overview

is whether a message in a given real-time stream should be transmitted by the router or dropped altogether. We enforce our (more general) dropping primitives at the granularity of multi-packet messages.

In-network dropping policies. CoDel [2] and RED [30] proactively drop packets on the onset of congestion to send an early signal to an endhost congestion controller (§2 shows how this can lead to link under-utilization). Octopus, instead, drops packets to directly adapt the transmitted content based on the network conditions and app-specified requirements.

Bhattacharjee et. al. proposed intelligent packet discard for MPEG transfers [14, 15] as a usecase of active networking. The goal was to ensure that a buffer overflow discards lower priority video frames. Octopus differs in its goal of minimizing latency by proactively discarding messages (before the buffer fills up) using more direct triggers in the form of new message arrivals and instantaneous link capacity. We evaluate the significance of doing so in §7. Bhattacharjee et. al.’s proposal further required the routers to maintain app-specific logic. In contrast, Octopus routers are app-agnostic, and implement parameterized primitives to enforce app-specified policies.

Video adaptation at endhosts. Most current schemes for real-time video streaming adapt quality or frame rate at the endhosts, relying on a congestion control algorithm to estimate network capacity [21, 31, 40, 42, 47, 73]; this includes schemes that use SVC [58, 67] but drop higher quality layers at the endhost. Inaccuracies in bandwidth estimation at the endhost may result in sub-optimal throughput or higher latencies (§2).

4 Octopus Design

As depicted in Figure 3, Octopus is a cross-layer system consisting of the following elements:

Octopus-aware Application. An app specifies its desired dropping policy (as per its requirements and stream encoding format) to the underlying Octopus transport in the form of parameters for Octopus’ *dropping primitives* (detailed in §4.1). The app specifies these parameters for individual *messages*

(where a message may contain one or more packets, and is the unit of packet drops in Octopus).

This seemingly increases the burden on app development. Nonetheless, app-layer frameworks that support mechanisms to encode real-time streams and adapt their content based on estimated bandwidth availability already exist (e.g. WebRTC for real-time videos[7]). We envision that rather than changing individual apps, one would extend such frameworks to exploit Octopus.

In order to fully exploit Octopus, a real-time stream must be able to tolerate in-network packet drops. For instance, in a single-layered video codec that uses every single frame as a reference to encode the next frame (as in H265 [62] and VP9 [3]), a drop in one frame will disable decoding all subsequent frames. We show how existing multi-layer extensions of such codecs (e.g. SVC [4, 59]) can be effectively used with Octopus in §6.

Octopus Transport. The underlying transport (detailed in §4.2) encodes the dropping policies (that the app specifies in the form of per-message parameters) in individual packet headers. It paces out the data packets sent into the network using BBR’s congestion control logic. This ensures that the data transfer rate is limited to the peak capacity of the bottleneck cellular link, and that the Octopus traffic competes fairly with the rest of the wide-area traffic. If the pacing rate is slower than the rate at which an app generates data, messages get queued up in the transport buffer. Octopus implements its message dropping primitives at the transport buffer (as per the app-specified parameters). This direct and timely content adaptation in the transport buffer mitigates the need for additional app-layer content adaptation strategies that are based on feedback from the transport.² It acts as a first-level of content adaption at the endpoint itself, and is sufficient if the network bandwidth is stable and matches the pacing rate.

Octopus Router. Given the inherent inaccuracy in estimating volatile link bandwidth, and the relatively aggressive congestion controller (BBR) used by Octopus, the pacing rate at an endpoint might be higher than what the cellular link can support. The Octopus router logic (§4.3) kicks in to adapt stream content and minimize in-network delays in such cases. It implements the Octopus dropping primitives, parses the packet headers to read app-specified parameters, and enforces the desired dropping behaviour.

4.1 Dropping Primitives

A real-time data stream consists of a series of temporal data units, each corresponding to a point in time. Generalizing the terminology used for video streams, we refer to each such temporal unit as a frame. Each frame has a base layer

²We provide a direct comparison of Octopus’ endpoint content adaptation (without the in-network logic) with other endpoint-based solutions in §7.1.

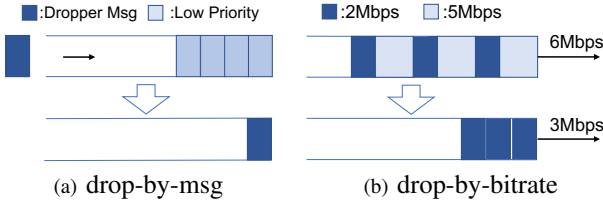


Figure 4: Two dropping conditions for Octopus

at a specific quality level, and may optionally have additional quality-enhancing layers. If the link bandwidth is larger than the incoming rate of the stream, the link can sustain the stream and no frames get queued up. If not, multiple frames get queued up at the link buffer, and we need to adapt the buffered content by dropping packets in order to sustain the stream. There are two ways in which the content of real-time streams can be adapted – (i) reducing the temporal resolution (or the frame rate) by dropping entire frames, and, (ii) if supported, reducing the spatial resolution (or data quality) by dropping one or more quality enhancing layers within a frame. Such content adaptation must further take the stream encoding (or the frame dependency structure) into account – if a “reference” frame/layer is dropped, subsequent frames/layers that semantically depend on it cannot get decoded.

We define a *message* as the atomic granularity at which Octopus routers drop data packets in a stream. A message would correspond to an entire frame if content is adapted solely via reducing the temporal resolution. In streams that also support adapting spatial resolution, a message would correspond to a quality layer in each frame. An app identifies its message boundaries, and specifies its dropping policies (as per its requirements and stream encoding format) in terms of per-message parameters supported by Octopus’ dropping primitives. We now detail these primitives.

Dropping Condition 1: Newer Message Arrival. In our first primitive, the arrival of a newer (more important) message triggers dropping (a subset of) staler queued-up messages. Octopus tags each message with app-specified (i) priority value (*msg_priority*), where a higher value implies lower priority, and (ii) a *drop_flag* with an associated *priority_threshold* value. When a new message is enqueued at the buffer, if its *drop_flag* is set, it triggers dropping all previously queued up messages in the same stream which have $\text{msg_priority} \geq \text{priority_threshold}$. We refer to the messages with the *drop_flag* set as *dropper messages*, and refer to this primitive as *drop-by-msg* primitive.

An app can configure the message boundaries and the primitive’s parameters to specify which messages’ arrival will drop which subset of queued-up messages. For streams with independent frames (e.g. a stream of images), simply setting

the *drop_flag* in each message (frame) will maximize freshness. If a stream requires fixed temporal resolution but allows tuning spatial resolution, the app can configure the message boundaries and parameters to only drop the queued-up quality-enhancement layers upon the arrival of a new frame. Or, based on the stream encoding, an app can configure the parameters to avoid dropping a reference frame upon the arrival of a new frame dependent on it.

In general, a queue build-up of two or more frames is a good indicator of the inability of the link to sustain the incoming stream. The drop-by-msg primitive is designed to immediately react to such queues in order to minimize queuing delay. However, small transient queues of multiple frames may build-up when there is a mismatch between the average and the instantaneous rate of the incoming stream due to differences in frame sizes. Our second primitive is designed to provide increased tolerance towards such transient queues.

Dropping Condition 2: Bandwidth Lower than Data Bitrate. In certain stream encodings, the frame sizes may differ significantly. For example, in a layered video codec, the size of first reference frame in each “group of pictures” (on which subsequent frames in the group depend) can be 4X larger than the non-reference frames. Even if the link bandwidth is sufficient to sustain the average bitrate across several frames, a transient queue might build-up while serving the larger (reference) frames. If the dropper messages in drop-by-msg primitive are spaced very closely, the quality-enhancement layers in the reference frame might get dropped in the transient queue causing the subsequent dependent frames to be decoded at the lowest quality level (even though the link bandwidth was sufficient to sustain the average bitrate of high quality layers). On the other hand, if the dropper messages are spaced too far apart (or configured to avoid dropping reference layers), and the link bandwidth is indeed smaller than the average bitrate of higher-quality layers, it could happen that by the time a suitable dropper message arrives, the higher-quality layers (that should have been dropped) have already left the queue after having contributed to a large queuing delay for the remaining frames.

To handle such scenarios, we additionally need a dropping condition that is directly based on the available link bandwidth, and does not rely on subsequent dropper messages. Our second primitive provides this.

An app can tag each message with a *bitrate_threshold*.³ Octopus drops a message if the stream is currently being served at a bandwidth *BW* that is less than its *bitrate_threshold*. We refer to this primitive as *drop-by-bitrate* primitive. It allows an app to specify different *bitrate_thresholds* for different spatial layers in the stream, thus enabling the Octopus buffer to

³It can use its knowledge of the stream encoding and data rate for this.

directly determine whether a spatial layer should be dropped or transmitted based on the available link capacity.

Summary. Octopus supports two conditions to drop messages. The combination of the two primitives provides an expressive mechanism for real-time apps to specify different content adaptation policies. We exemplify their usage in §6.

4.2 Transport Design

API. An app conveys its dropping policies via Octopus’ transport interface. In particular, the app conveys its atomic message boundaries to the transport, and for each message, specifies its stream_id (which explicitly identifies the stream that the message belongs to), msg_priority, and the dropping parameters (that include the drop_flag, the associated priority_threshold, and the bitrate_threshold).

By default, Octopus transport sets all dropping parameters in a message to zero, if not explicitly configured by the app, that disables any content adaptation.

Encoding dropping policies. Octopus transport tracks per-stream message sequence space. Upon receiving a new message from the application, it increments the corresponding msg_id counter, packetizes the data, and encodes the msg_id, priority, and parameters in designated packet header fields. The header fields additionally carry information about whether the packet is the first, last, or only packet of the message.

Transport buffer management. Similar to TCP, Octopus transport enqueues the packets in a send buffer, until they can be sent out to the lower layers. As mentioned earlier, it enforces the same message dropping policies in this transport buffer as the one enforced by the router buffer (described in more details in §4.3).⁴ It uses the bandwidth estimated by the congestion control algorithm as the current available bandwidth for the drop-by-bitrate primitive.

Loss handling and message delivery. Octopus transport is unreliable (future extensions can support partial reliability). The receiver acknowledges received data (required for congestion control), although no packets are retransmitted. As soon as a message is completely received, the Octopus receive-side transport delivers it to the application, irrespective of whether prior messages have been delivered.

Congestion control. Octopus requires congestion control to ensure that the data transfer rate is limited to the peak capacity of the bottleneck cellular link, so as to not overwhelm the rest of the network. Moreover, there might be scenarios where the bottleneck lies elsewhere in the network (e.g. at a

⁴Octopus design can be naturally extended to scenarios where the bottleneck is at the upload link on the user device (and not at the download link on the cellular base-station). The endhost could use a back-pressure based mechanism (similar to TCP small queues [28]) to restrict the transport from sending more data when the (small) NIC buffer is full. The Octopus logic implemented at the transport buffer would then appropriately drop messages. We leave a detailed implementation of this to future work.

Algorithm 1 Octopus’ packet dropping logic

```

variable dropper_msgs_, msg_in_drop_
procedure ENQUEUE(packet)
    sid ← packet.streamID()
    if packet.hasDropFlag() and packet.isTail() then
        threshold ← packet.priorityThreshold()
        dropper_msgs_[sid][threshold] ← packet.msgID()
    end if
    buffer_.push(packet)
end procedure
procedure DEQUEUE(void)
    packet ← buffer_.pop()
    msgid ← packet.msgID()
    sid ← packet.streamID()
    if packet.isHead() then
        prio ← packet.priority()
        latest_dropper ← max(dropper_msgs_[sid][0],
            ..., dropper_msgs_[sid][prio])
        isdrop ← msgid < latest_dropper
        or packet.bitrateThreshold() > BW[sid]
        if isdrop then
            msg_in_drop_[sid] ← msgid
        end if
    end if
    if msg_in_drop_[sid] = msgid then
        return Drop(packet)
    end if
    return packet
end procedure

```

legacy switch that does not support Octopus), requiring Octopus to compete fairly with the cross-traffic. We incorporate BBR’s congestion control logic in Octopus transport. BBR, by design, tracks the maximum packet bandwidth and the minimum RTT over a configurable period of time, and uses this to compute the delivery rate and the congestion window. This enables BBR to continue sending at the peak cellular capacity, without getting perturbed by transient dips in available bandwidth. As shown in §2, this does come at the cost of high queueing delays which we handle through our in-network dropping policies.

4.3 Router Design

An Octopus router at a cellular base-station enforces the dropping primitives, as per app-specified policies encoded in packet headers. Cellular routers already maintain separate queues for individual users [19, 32, 69]. We further assume that a user’s real-time traffic is isolated from their non-realtime traffic (standard mechanisms for doing so already exist in cellular networks[9, 19]).

Octopus requires the router to track the available bandwidth BW for each (per-user) queue. This is often directly available in cellular links [1, 33]. It can also be measured at the router by tracking the rate at which packets are dequeued and transmitted, as we do in our experiments (§5). If a given user downloads multiple real-time streams, the router computes the max-min fair rate BW_i for each stream i from the observed per-stream arrival rate and the overall rate BW at which the user’s queue is served.

Algorithm 1 shows the pseudo-code for the packet dropping logic. For each stream, the router maintains a table indexed by the `priority_threshold` that records the `msg_id` of the latest dropper message corresponding to that threshold. It updates this table when enqueueing the tail packet of a dropper message. When the head packet of a message from stream i is dequeued, the router marks this message to be dropped if: (i) its `bitrate_threshold` is higher than BW_i , or (ii) its `msg_priority` is greater than or equal to the `priority_threshold` of all dropper message in the queue that belong to the same stream. If a message is marked for drop, all the following packets belonging to it are dropped during dequeuing. To avoid starvation, the router does not drop a message that is in transmission (i.e. one or more of whose packets have been transmitted).

Notice that Octopus requires maintaining very modest amount of per-stream state in the routers, which remains constant with number of packets or messages. It only grows with the number of priority threshold levels in a stream – we expect this number to be small for most usecases (§6), and it is restricted to 8 in our prototype.

5 Prototype Implementation

Octopus Transport. We implement Octopus transport in 3000 LoC by extending the UDT framework, a user-space transport protocol over UDP [34]. This includes implementing BBR’s congestion control logic. Our prototype uses UDT’s app-layer header to encode message properties and dropping policies, which take 12 bytes. An actual deployment can instead make use of IPv4 options or IPv6 extension fields to encode Octopus parameters.

Octopus Router. We implement Octopus’ in-network logic in srsRAN[32, 63], an open-source software cellular platform for 5G and LTE radio access network (RAN). Our changes to srsRAN fit within 420 LoC.

The network protocol stacks of the 5G/LTE base station in srsRAN are shown in Figure 5. Specifically, the RLC (radio link control) layer instantiates an entity to manage an isolated logical queue for each connected user. We implement the Octopus’ dropping primitives and maintain runtime data in the RLC entity. In the ingress stage, the RLC entity parses the app-layer headers of incoming packets, and accordingly updates the table of latest dropper messages. In the egress stage, Octopus determines whether the current message is to be dropped

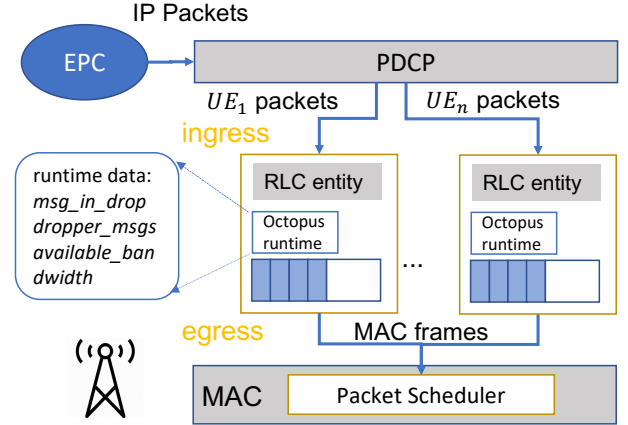


Figure 5: eNB/gNB protocol stack with Octopus runtime

based on the dropping conditions, and drops packets belonging to it in that case. For the drop-by-bitrate primitive, we track the bandwidth availability by computing the dequeuing rate over a sliding time window of 50ms (discounting the idle periods when the queue is empty).

We deploy the srsRAN platform on a server with eight Intel Xeon E5 cores. The software-based srsRAN platform can support a data-rate of up to 75Mbps – this remained unaffected by adding Octopus logic. Octopus’s dropping logic is light-weight, and can be easily supported in other hardware-based RAN platforms (we back this claim by discussing the feasibility of implementing Octopus on P4 in Appendix A).

6 Case Studies

We evaluate Octopus using three case studies involving real-time video streaming with frame rate adaptation (§6.1) and quality adaption (§6.2), and live volumetric video streaming (§6.3). We focus on real-time 2D/3D video streaming in our case studies due to their relative popularity across apps (in conferencing, gaming, VR, surveillance, robotics, etc) and due to the existence of comparative baselines. One can design similar policies to exploit Octopus for other forms of real-time streams. In this section, we present our basic results, comparing Octopus policies with state-of-the-art transmission schemes[31, 37, 73], and present a more in-depth evaluation in §7.

Experiment Testbed. Our testbed involves a sender and a receiver node (both running Octopus transport on UDT) communicating via the srsRAN platform. We emulate cellular link bandwidth and delay on the downlink from the base station to the receiver.⁵ For the first two case studies, we experiment with bandwidth traces from three different LTE cellular providers (Verizon, T-Mobile, and ATT)[69]. The

⁵For this, we use the cellular downlink traces [69] as input to set the maximum MAC frame size in srsRAN every TTI.

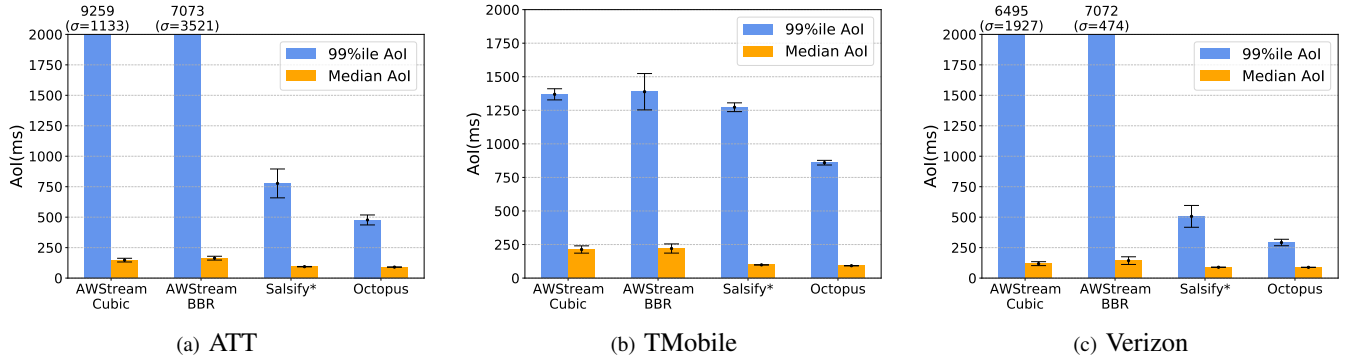


Figure 6: Median and 99%ile AoI in different LTE download network traces with RTT 60ms (averaged over 5 videos, with error bars showing standard deviation).

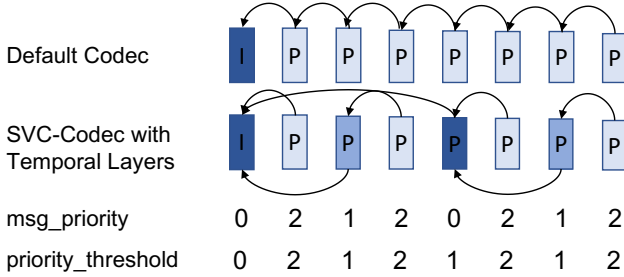


Figure 7: Single-layered video codec (top) and SVC with three temporal layers (bottom).

video sources are five different videos taken from MOT17 and MOT20 datasets [24, 49].

For the third case study involving volumetric videos, we experiment with two different 5G cellular download traces [55]. To support higher 5G data-rates in this case-study, we replace our srsRAN platform with Mahimahi network emulator [53], and implement Octopus’ router logic in Mahimahi. The volumetric video sources are three videos in point cloud format taken from CMU panoptic dataset [43].

We experiment with three different RTTs (20ms, 60ms, and 120ms) for each case-study. For brevity, we only present results with 60ms RTT (we see similar trends at other RTTs, and present results with RTT 120ms in §7 and appendix).

6.1 Real-time Video with Frame Rate Adaptation

Our first case study considers the requirement where the freshest video frame must be delivered at fixed quality (e.g. for applications that require processing the received video using an ML algorithm).

Video Encoding. Commonly used video codecs (e.g. H.264 [66] and VP9 [3]) encode video frames in chunks called “group of pictures” (GoP). As shown in Figure 7 (top), the first frame in each GoP (the I-frame) is intra-coded and can be decoded independently. Each subsequent P-frame only encodes the

delta from the previous frame. The successful decoding of a P-frame at the receiver therefore requires successful delivery of all previous frames in the GoP. This limits the tolerance to in-network packet drops.

To better exploit Octopus, we make use of multiple temporal layers supported by scalable video codec(SVC)[4, 6, 59]. Here, we apply VP8-SVC with three temporal layers. Figure 7 (bottom) shows the dependency structure between frames. Frames marked with priority value i serve as reference only for frames with priority value $j > i$, and can be dropped upon the arrival of a new frame with priority_threshold $k \leq i$, without affecting any subsequent frames. The usage of VP8-SVC introduces slight overhead – the average frame size is 15%-18% larger than that encoded in default VP8. Our results show how Octopus improves overall performance in spite of these overheads, in comparison with baselines that use the default codec.

Dropping Policy. Using the video codec described above, we treat each frame as a single message, and only make use the drop-by-msg primitive. We set the drop_flag in every message. Figure 7 shows the msg_priority, and priority_threshold that we set for each message. The bitrate_threshold is set to the default value of zero to disable drop-by-bitrate primitive.

Baselines. We compare Octopus with two state-of-the-art schemes for real-time video transmissions: (i) AWStream [73], configured to adapt frame rate based on the bandwidth estimated by the underlying transport (we experiment with both TCP Cubic and BBR). We use the default VP8 encoding for the video. (ii) Salsify [31], modified to solely tune the frame rate keeping the frame quality fixed (we refer to this as Salsify*). As in the original Salsify design, it uses Sprout’s EWMA-based congestion control mechanism (a more aggressive variant of Sprout [69]), and a functional codec based on VP8 encoding. We encode the videos for all three schemes with a fixed quantization level of 17.

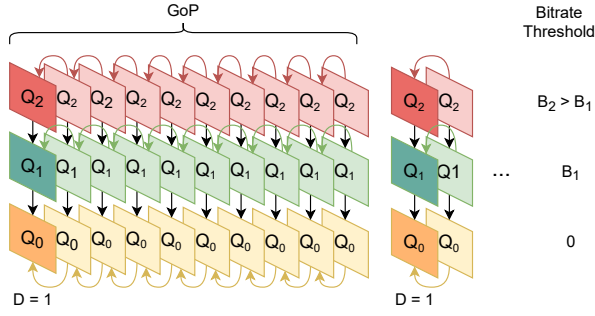


Figure 8: SVC encoding with three quality layers, and the dropping primitive parameters.

Metric. We use “age of information” (AoI) [46] to capture freshness as the time elapsed since the latest frame delivered at the receiver application was sent out by the sender application (lower AoI implies higher freshness). To capture the worst-case freshness, we measure the AoI just before a frame is received, and compute the 99%ile and median values across all frames in a video. AoI can be high either due to high queuing delays or low frame rate (or both).

Results. As shown in Figure 6, Octopus outperforms AWStream and Salsify*, in spite of using a less efficient encoding strategy. The tail AoI with Octopus is 1.6-18 \times lower than that of AWStream. We found that AWStream (designed for more stable WAN bandwidth) is overly conservative in increasing its sending rate (upgrading to a higher throughput configuration only after its application buffer has been empty for 2s). The tail AoI with Octopus is 1.5-2 \times lower than Salsify*’s - Salsify* suffers from higher tail latencies and lower link utilization due to slower reaction to changing network capacity as compared to Octopus.

6.2 Real-time Video with Quality Adaptation

Many real-time apps (e.g. video conferencing and live streaming) allow tuning the quality of the video content to sustain stable FPS with low latency. Our second case study considers this requirement.

Video Encoding. We exploit support for multiple spatial (quality) layers in SVC for quality adaptation with Octopus.⁶ Figure 8 shows how frames are encoded in SVC with 3 spatial layers (depicted as Q_0 , Q_1 , and Q_2 from lowest to highest). The decoding of a higher layer frame depends on the successful decoding of all lower layers and the corresponding layer of the previous frame.

In our SVC-based Octopus application, we fix the number of quality levels to 3, and use the bandwidth estimation (B) provided by the underlying Octopus transport to dynamically

adjust the encoding quality levels for each GoP.⁷ More specifically, quality Q_2 is configured such that its cumulative target bitrate is $B_2 \approx B$, Q_1 is configured to a cumulative bitrate of $B_1 \approx 0.5B$, and Q_0 is configured to a bitrate $B_0 \approx 0.2B$. We reduce the GoP size to 10 frames. This introduces a slightly higher overhead, but allows faster switching across quality levels.

Dropping Policy. We use the drop-by-bitrate primitive, treating each layer of each frame as an individual message. We mark the messages corresponding to quality Q_0 , Q_1 and Q_2 with bitrate_thresholds of zero, B_1 and B_2 respectively.

Overall, this policy achieves the desired trade-off in quality, throughput and message latency. However, it has a few caveats: (1) It may result in high queuing when the bandwidth is lower than B_0 (the required bitrate for the lowest quality frames). We handle this by using our drop-by-msg primitive, and setting the drop_flag in the first Q_0 message in each GoP. With priority_threshold of zero, this triggers a drop in all queued up frames of the previous GoP. (2) There might be scenarios where the bandwidth increases after some of the Q_2 or Q_1 messages towards the beginning of a GoP have been dropped. Transmission of Q_2 messages in the GoP that are then enqueued is wasteful as they cannot be decoded at the receiver. Nonetheless, we observe that if the bandwidth is high enough to sustain their bitrate, transmission of these messages do not generally block transmission of newer frames in the stream. Moreover, by limiting the GoP to 10 frames, we limit the scope of such wasted frame transmissions.

Baselines. We compare Octopus for this usecase with: (i) AWStream, configured this time to adapt video quality, (ii) Unmodified Salsify.

Metric. We measure the video quality using SQI-SSIM[27, 56] – it computes the quality of each decoded frame using structural similarity(SSIM) [39, 75], and the quality of each undecoded (or dropped) frame as the product of the SSIM of the last available frame and an exponential decay function. The resulting video QoE score is the average quality across each (decoded and undecoded) frame that was sent by the sender app. We also record the latency of each delivered frame. It’s desirable to achieve high SQI-SSIM and low latency.

Results. As shown in Figure 9, Octopus achieves higher average SQI-SSIM with lower tail latency than the baselines (the median latency, shown in Appendix, is similar across different schemes). Octopus achieves 14-31% higher SQI-SSIM than AWStream, with 2-50 \times lower tail latency. The difference in SQI-SSIM stems from AWStream’s conservative behaviour when upgrading to higher throughput configuration. AWStream’s tail latency is relatively high due to poor

⁶Future work can explore using other layered codecs, e.g. neural video codec[22].

⁷We found that a frame with up to three SVC layers can be decoded within 10ms using a single-threaded code.

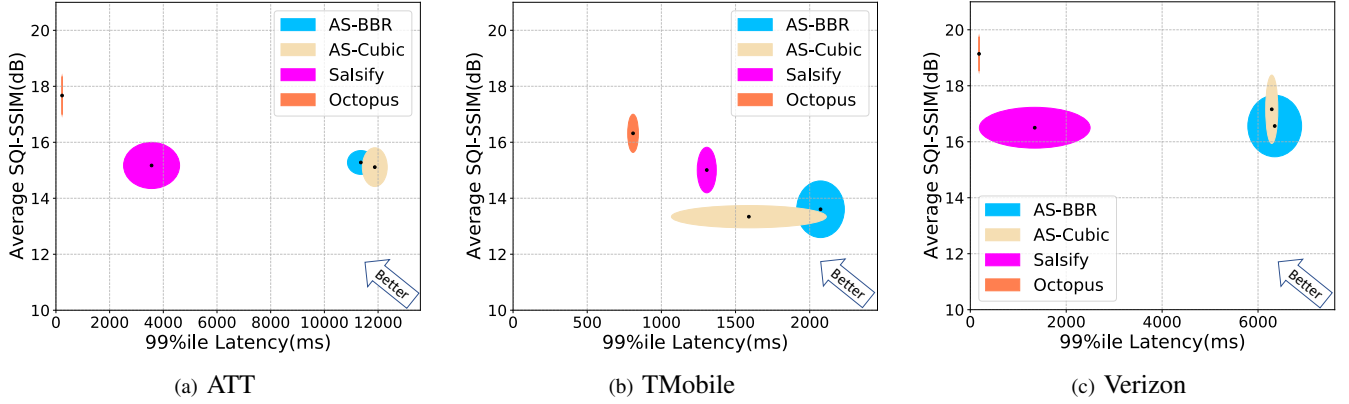


Figure 9: The 99%ile tail latency v.s. video quality of Octopus and other baselines in different LTE download traces with RTT 60ms. The axes of the ellipse reflect the standard deviations in SQI-SSIM and tail latency.

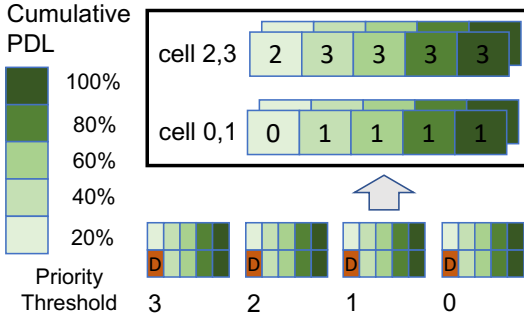


Figure 10: The upper graph shows a volumetric video frame with four cells, and each cell with five layers. The lower graph shows dropper messages and their priority thresholds.

reaction when link capacity suddenly drops to very low values. Octopus achieves 17% higher SQI-SSIM than Salsify, with 1.6-10 \times lower tail latency. The difference in SQI-SSIM largely stems from the inefficiency of the functional VP8 codec used in Salsify. The difference in tail latency stems from Octopus’s faster reaction to sudden drops in bandwidth.

6.3 Real-time Volumetric Video Streaming

Real-time volumetric streaming enables viewers to watch videos in six degree of freedom (6DoF), and is becoming popular in education, entertainment, and healthcare. We look at how Octopus can adapt the quality of bandwidth-intensive volumetric streams to minimize delay while trying to sustain a stable frame rate.

Video Encoding. Uncompressed volumetric video frames are represented as point clouds which record the attributes such as coordinates and colors of every point. A frame is often spatially segmented into multiple cells, and each cell can be independently encoded and decoded [37, 48]. This

segmentation enables the server to stream a subset of cells or adapt the point density level (PDL) of cells based on the viewer’s current viewport to significantly reduce network bandwidth requirement.

Figure 10 shows how we encode a volumetric frame. In our experiments, every video frame is segmented in four cells. Instead of encoding every cell with a specific PDL, we further divide the origin cell into five layers, each comprising 20% points and encoding every layer independently, so that Octopus can safely drop specific layers in a cell to adapt its PDL. This results in only 10%-12% overhead in terms of bandwidth usage which, as our results show, is more than compensated by Octopus’ fast reaction to bandwidth changes compared to the baseline.

Dropping Policy. Based on the Occlusion Visibility(OV) and Distance Visibility(DV) adaptive streaming approaches from ViVo [37], we first drop layers of occluded cells, and then drop higher density layers of non-occluded cells, as queues start building up. For simplicity we assume the viewport is fixed and cell 0 and cell 1 are front cells and cell 2 and cell 3 are occluded cells (we can dynamically update the cells priority for changing viewport using the viewport movement and prediction model from ViVo).

We apply drop-by-msg primitive, and treat each layer inside a cell as an individual message. The message priority for each such layer is indicated in Figure 10. We set the drop_flag in the first layer of the non-occluded cell 0 in every frame. The drop_thresholds in these dropper messages are set to a repeating pattern of 3, 2, 1, and 0, which enables the smooth adaptation of cell PDLs in buffer.

Baselines. We compare Octopus with ViVo in this usecase. Since the source code of ViVo is unavailable, we implement a version to our best knowledge. Here, the ViVo client uses a throughput-based rate adaptation algorithm[41] to estimate

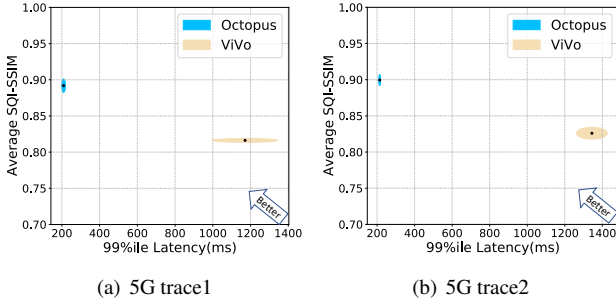


Figure 11: The 99% tail latency v.s. volumetric video quality of Octopus and ViVo in two 5G traces with RTT 60ms.

the link capacity, and determine the PDL of occluded cells and front cells to fetch.

Metric. Similar to §6.2, we use SQI-SSIM to compute the quality of received volumetric video frames, and 99% frame delivery tail latency to capture freshness of frames. To calculate the SSIM, we leverage the mappings from cell PDLs to SSIM perceived by viewers at a given distance developed by ViVo. In the experiment, the default distance between the viewport and cells is 2.5m.

Results. From Figure 11, Octopus achieves 9% percent higher average SQI-SSIM and 83% lower tail latency than ViVo. The reason that ViVo has lower frame quality stems from its conservative rate adaptation algorithm, which uses the harmonic mean of the download rate of previous 20 video frames as the capacity estimate for the next frame. ViVo’s tail latency is relatively high because TCP reliably delivers all packets even when the real network bandwidth suddenly drops below the estimate.

7 Detailed Evaluation

We use our case-study in §6.2 for a more in-depth evaluation of Octopus. For brevity, we only present results with Verizon download trace at RTT 120ms (we see similar trends with other traces). We use our srsRAN testbed for the results in §7.1, and Mahimahi emulator (that allows for greater configurability in experimental scenarios and baselines) for the remaining experiments.

7.1 Decoupling the impact of Octopus Endpoint Logic

We now evaluate the performance impact of Octopus endpoint’s logic in isolation. For this, we use Octopus transport protocol as it is, but disable the Octopus router logic. This effectively models BBR using Octopus logic for transport buffer management and app content adaptation. We refer to this scheme as OctoBBR.

Figure 12(a) compares OctoBBR with Octopus, as well as the baselines described in §6. There are two key takeaways from these results:

- (i) Octopus performs better than OctoBBR. Octopus achieves a more desirable trade-off than OctoBBR with 75% lower tail latency and only 3% lower SQI-SSIM. This shows that in-network content adaptation (based on more timely and accurate knowledge of link capacity and queue build-up) is useful.
- (ii) OctoBBR performs better than the state-of-the-art endpoint-based solutions (Salsify and AWStream). This highlights the benefits of direct content adaptation at the endpoint’s transport buffer by dropping messages using Octopus’ primitives when there’s a mismatch between the application sending rate and the pacing rate of transport protocol.

7.2 Comparison with Priority-based Message Dropping

We next compare Octopus’ in-network message dropping logic with a simpler priority-based message dropping mechanism (inspired from [14, 15]). With this mechanism, when the router buffer is full, and a new message with priority p arrives, instead of dropping the incoming message, the router drops all queued up messages with lower priority (i.e. having priority value $> p$). We set highest priority 0 for base (Q_0) layer, followed by priority 1 for Q_1 , and then priority 2 for Q_2 .

Figure 12(b) compares Octopus with the priority-based dropping scheme described above (represented as PDrop). We fix the buffer size to 375KB for Octopus, and use varying buffer sizes for PDrop. We find that PDrop is sensitive to buffer sizes. Larger buffer size results in fewer message drops, and larger latency. A small buffer size, on the other hand, results in significantly lower video quality. Packet delay thresholds or deadlines would be similarly difficult to tune. Octopus primitives are able to react faster and more appropriately by triggering drops directly based on message arrival and link capacity, instead of relying on a buffer threshold. This allows Octopus to achieve a more desirable trade-off.

7.3 Competing Backlogged Flow at a Legacy Switch

We emulate a legacy (non-Octopus) switch with a static link bandwidth of 12Mbps. In addition to the real-time stream, we generate a competing backlogged TCP (BBR) flow that shares the switch buffer. Figure 12(c) presents the results of Octopus and comparative baselines in this scenario. With the Octopus router logic disabled for the legacy switch, only the Octopus endpoint logic kicks in (which, in line with §7.1 is represented as OctoBBR). Overall, we find that OctoBBR achieves the most desirable trade-off between SQI-SSIM and latency. We find that Salsify (using Sprout as the underlying transport) competes poorly with the backlogged TCP flow, utilizing less than its fair share of the link capacity, which in

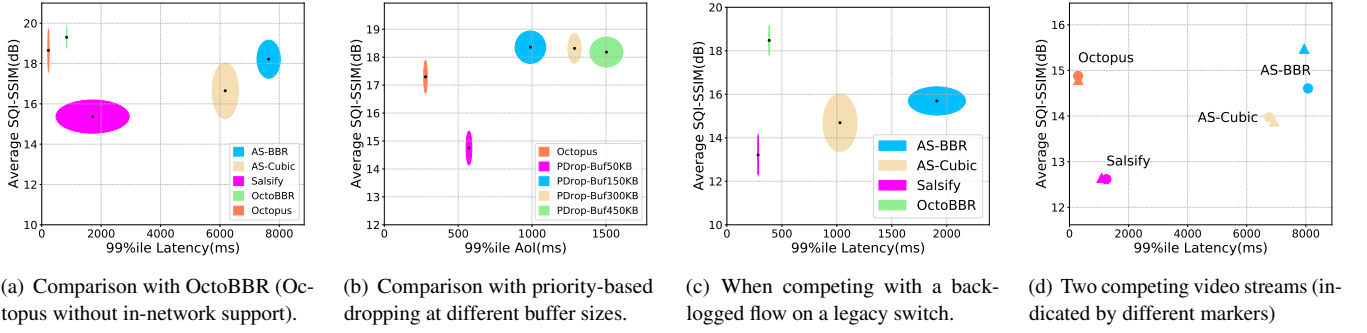


Figure 12: The 99%ile tail latency v.s. video quality of Octopus and other baselines for real-time video under different scenarios on the Verizon trace with 120ms RTT.

turn reduces the video quality. OctoBBR competes fairly with the backlogged flow, allowing it to achieve 40% higher SQI-SSIM than Salsify. The graph comparing the link utilizations achieved by Salsify and OctoBBR is shown in Appendix C. Both Salsify and OctoBBR see similar increase in in-network delay due to the competing flow, but OctoBBR sees slightly higher self-inflicted delay as it is able to send more messages into the network (that the legacy switch does not drop). This results in 18% higher tail latency in OctoBBR compared with Salsify. AWStream has lower video quality (due to the aforementioned conservative app behavior, which results in low link utilization) and larger tail latency (due to higher queuing delay in the endpoint’s transport buffer).

We also evaluated a scenario with multiple bottlenecks, one at a legacy switch and another at an Octopus-enabled cellular base-station. We present those results in Appendix D.

7.4 Competing real-time streams sharing Octopus buffer

We next evaluate a scenario with two real-time video streams sharing the same router queue. For the drop-by-bitrate condition, the router computes the max-min fair rate BW_i for each stream i from the observed per-stream enqueueing rate and the overall rate at which the queue is served. We use the policy from §6.2 for both streams. Figure 12(d) compares Octopus with Salsify and AWStream (the result for each video stream is denoted using two different markers). We find that Octopus achieves higher SQI-SSIM and lower tail latency for both video streams, as compared to Salsify and AWStream. This shows that Octopus can appropriately handle multiple real-time streams, when the dropping parameters in each stream are configured to minimize the self-inflicted delay.

8 Scope and Limitations

The goal of our work was to present a new design point for controlling congestion that is based on in-network content adaption, and show the promise of this approach. We acknowledge that our approach requires changes at both the endpoints

and the cellular routers, making it difficult to deploy immediately. We list a few other limitations of our work below:

Applicability. Our approach does not entirely replace the need for feedback-based controllers – it is well-suited only for those apps that can support in-network content adaption.

On generality of our primitives. While our primitives can seemingly capture a range of requirements for real-time apps, we are yet to formally analyze their expressiveness.

Coordination via packet headers. Octopus needs 12 bytes of header space to convey the per-message dropping parameters. While our prototype uses application-layer headers, an actual deployment may need to use other alternatives (e.g. IP options/extensions). Diving into the feasibility of these alternatives is beyond the scope of our work.

Competition with buffer-filling cross-traffic. We assume that a user’s real-time traffic is isolated from their non-realtime traffic using standard mechanisms [9, 19]. We find that in the absence of such isolation, Octopus’ dropping logic competes poorly with flows that aggressively fill up the network buffer.⁸ Such a fate is fundamental to any scheme that is designed to react fast to bandwidth variations, and isolation from buffer-filling cross-traffic is therefore a common assumption that is also made by prior work [31, 33, 69].

9 Conclusion and Discussion

This paper presented Octopus, a system designed to achieve high throughput and low latency for real-time transmissions over cellular networks. Typical real-time apps adapt their content (data quality and frame rate) based on the network bandwidth estimated by the endpoint transport. Octopus allows these apps to send data aggressively, and to instead specify how content can be adapted by the lower layers using per-message parameters. Octopus transport and router logic implement generalized primitives to drop messages as per app-specified parameters when a queue build ups or link

⁸Disabling Octopus’s in-network logic and relying on its transport logic still outperforms state-of-the-art baselines in such scenarios, as discussed in §7.3.

bandwidth reduces. This allows Octopus to react in a timely manner, and perform significantly better than state-of-the-art.

Our work leaves several interesting directions open for future research. For example, how can application frameworks be designed to better exploit a system like Octopus? Can this approach be extended to other scenarios, e.g. for datacenter workloads? How well do Octopus' primitives generalize to other usecases? etc.

References

- [1] 2010. 3GPP technical specification for lte. https://www.etsi.org/deliver/etsi_ts/132400_132499/132450/09_01.00_60/ts_132450v090100p.pdf.
- [2] 2011. sfqCoDel. <http://www.pollere.net/Txtdocs/sfqcodel.cc>.
- [3] 2017. VP9 Video Codec. <https://www.webmproject.org/vp9/>.
- [4] 2020. vp9_spatial_svc_encoder. https://chromium.googlesource.com/webm/libvpx/+master/examples/vp9_spatial_svc_encoder.c.
- [5] 2021. Understanding Packet Loss Priorities. https://www.juniper.net/documentation/en_US/junos/topics/concept/cos-packet-loss-priority-understanding-security.html.
- [6] 2022. Scalable Video Coding (SVC) Extension for WebRTC <https://www.w3.org/TR/webrtc-svc/>. <https://www.w3.org/TR/webrtc-svc/>.
- [7] 2022. WebRTC: Real-time communication for the web <https://webrtc.org/>. <https://webrtc.org/>.
- [8] Admin. 2021. 20 Astonishing Video Conferencing Statistics for 2021. <https://digitalintheround.com/video-conferencing-statistics/>.
- [9] Mehdi Alasti, Behnam Neekzad, Jie Hui, and Rath Vannithamby. 2010. Quality of service in WiMAX and LTE networks [Topics in Wireless Communications]. *IEEE Communications Magazine* 48, 5 (2010), 104–111. <https://doi.org/10.1109/MCOM.2010.5458370>
- [10] Mohammad Alizadeh, Albert Greenberg, David A. Maltz, Jitendra Padhye, Parveen Patel, Balaji Prabhakar, Sudipta Sengupta, and Murari Sridharan. 2010. Data Center TCP (DCTCP). In *Proceedings of the ACM SIGCOMM 2010 Conference* (New Delhi, India). Association for Computing Machinery, New York, NY, USA, 63–74. <https://doi.org/10.1145/1851182.1851192>
- [11] Mohammad Alizadeh, Shuang Yang, Milad Sharif, Sachin Katti, Nick McKeown, Balaji Prabhakar, and Scott Shenker. 2013. pFabric: Minimal Near-optimal Datacenter Transport. In *Proc. ACM SIGCOMM*.
- [12] Arjun Balasingam, Manu Bansal, Rakesh Misra, Kanthi Nagaraj, Rahul Tandra, Sachin Katti, and Aaron Schulman. 2019. Detecting If LTE is the Bottleneck with BurstTracker. In *The 25th Annual International Conference on Mobile Computing and Networking* (Los Cabos, Mexico) (*MobiCom '19*). New York, NY, USA. <https://doi.org/10.1145/3300061.3300140>
- [13] A. M. Bedewy, Y. Sun, and N. B. Shroff. 2019. Minimizing the Age of Information Through Queues. *IEEE Transactions on Information Theory* 65, 8 (2019), 5215–5232. <https://doi.org/10.1109/TIT.2019.2912159>
- [14] Samrat Bhattacharjee, Kenneth L Calvert, and Ellen W Zegura. 1997. An architecture for active networking. In *Proc. International Conference on High Performance Networking*. Springer.
- [15] Samrat Bhattacharjee, Kenneth L Calvert, and Ellen W Zegura. 1998. *Network support for multicast video distribution*. Technical Report. Georgia Institute of Technology.
- [16] Pat Bosshart, Dan Daly, Glen Gibb, Martin Izzard, Nick McKeown, Jennifer Rexford, Cole Schlesinger, Dan Talayco, Amin Vahdat, George Varghese, and David Walker. 2014. P4: Programming Protocol-independent Packet Processors. *ACM SIGCOMM Computer Communication Review* (2014).
- [17] Pat Bosshart, Glen Gibb, Hun-Seok Kim, George Varghese, Nick McKeown, Martin Izzard, Fernando Mujica, and Mark Horowitz. 2013. Forwarding Metamorphosis: Fast Programmable Match-Action Processing in Hardware for SDN. *SIGCOMM Comput. Commun. Rev.* (2013). <https://doi.org/10.1145/2534169.2486011>
- [18] Lawrence S. Brakmo, Sean W. O'Malley, and Larry L. Peterson. 1994. TCP Vegas: New Techniques for Congestion Detection and Avoidance. In *Proceedings of the Conference on Communications Architectures, Protocols and Applications* (London, United Kingdom). Association for Computing Machinery, New York, NY, USA. <https://doi.org/10.1145/190314.190317>
- [19] F. Capozzi, G. Piro, L.A. Grieco, G. Boggia, and P. Camarda. 2013. Downlink Packet Scheduling in LTE Cellular Networks: Key Design Issues and a Survey. *IEEE Communications Surveys Tutorials* (2013). <https://doi.org/10.1109/SURV.2012.060912.00100>
- [20] Neal Cardwell, Yuchung Cheng, C. Stephen Gunn, Soheil Hassas Yeganeh, and Van Jacobson. 2016. BBR: Congestion-Based Congestion Control. *ACM Queue* (2016).
- [21] Gaetano Carlucci, Luca De Cicco, Stefan Holmer, and Saverio Mascolo. 2016. Analysis and design of the google congestion control for web real-time communication (WebRTC). In *Proceedings of the 7th International Conference on Multimedia Systems*. 1–12.
- [22] Mallesham Dasari, Kumara Kahatapitiya, Samir R. Das, Aruna Balasubramanian, and Dimitris Samaras. 2022. Swift: Adaptive Video Streaming with Layered Neural Codecs. In *19th USENIX Symposium on Networked Systems Design and Implementation (NSDI 22)*. USENIX Association, Renton, WA, 103–118. <https://www.usenix.org/conference/nsdi22/presentation/dasari>
- [23] A. Demers, S. Keshav, and S. Shenker. 1989. Analysis and Simulation of a Fair Queueing Algorithm. *ACM SIGCOMM Computer Communication Review* (1989).
- [24] P. Dendorfer, H. Rezatofighi, A. Milan, J. Shi, D. Cremers, I. Reid, S. Roth, K. Schindler, and L. Leal-Taixé. 2020. MOT20: A benchmark for multi object tracking in crowded scenes. *arXiv:2003.09003[cs]* (March 2020). <http://arxiv.org/abs/1906.04567> arXiv: 2003.09003.
- [25] Mo Dong, Qingxi Li, Doron Zarchy, P. Brighten Godfrey, and Michael Schapira. 2015. PCC: Re-Architecting Congestion Control for Consistent High Performance. In *Proceedings of the 12th USENIX Conference on Networked Systems Design and Implementation*.
- [26] Mo Dong, Tong Meng, Doron Zarchy, Engin Arslan, Yossi Gilad, P. Brighten Godfrey, and Michael Schapira. 2018. PCC Vivace: Online-Learning Congestion Control. In *Proceedings of the 15th USENIX Conference on Networked Systems Design and Implementation*.
- [27] Zhengfang Duanmu, Zeng Kai, Kede Ma, Abdul Rehman, and Zhou Wang. 2016. A Quality-of-Experience Index for Streaming Video. *IEEE Journal of Selected Topics in Signal Processing* (Feb. 2016).
- [28] Eric Dumazet. 2012. TCP small queues. <https://lwn.net/Articles/506237/>.
- [29] Sally Floyd. 1994. TCP and Explicit Congestion Notification. *SIGCOMM Comput. Commun. Rev.* (1994). <https://doi.org/10.1145/205511.205512>
- [30] Sally Floyd and Van Jacobson. 1993. Random Early Detection Gateways for Congestion Avoidance. *IEEE/ACM Trans. Netw.* (1993).
- [31] Sadjad Fouladi, John Emmons, Emre Orbay, Catherine Wu, Riad S. Wahby, and Keith Winstein. 2018. Salsify: Low-Latency Network Video through Tighter Integration between a Video Codec and a Transport Protocol. In *Proc. USENIX NSDI*.
- [32] Ismael Gomez-Miguel, Andres Garcia-Saavedra, Paul D. Sutton, Pablo Serrano, Cristina Cano, and Doug J. Leith. 2016. SrsLTE: An

- Open-Source Platform for LTE Evolution and Experimentation. In *Proceedings of the Tenth ACM International Workshop on Wireless Network Testbeds, Experimental Evaluation, and Characterization* (New York City, New York) (*WiNTECH '16*). Association for Computing Machinery, New York, NY, USA, 25–32. <https://doi.org/10.1145/2980159.2980163>
- [33] Prateesh Goyal, Anup Agarwal, Ravi Netravali, Mohammad Alizadeh, and Hari Balakrishnan. 2020. ABC: A Simple Explicit Congestion Controller for Wireless Networks. In *Proc. USENIX NSDI*.
- [34] Yunhong Gu and Robert L. Grossman. 2007. UDT: UDP-Based Data Transfer for High-Speed Wide Area Networks. *Comput. Netw.* (2007).
- [35] Sangtae Ha, Injong Rhee, and Lisong Xu. 2008. CUBIC: a New TCP-friendly High-Speed TCP Variant. *ACM SIGOPS Operating System Review* (2008).
- [36] Cathy Hackl. 2021. The Future Of Live Events Begins In The Metaverse. <https://www.forbes.com/sites/cathyhackl/2021/07/20/the-future-of-live-events-begins-in-the-metaverse/?sh=57044a2d7ac9>.
- [37] Bo Han, Yu Liu, and Feng Qian. 2020. *ViVo: Visibility-Aware Mobile Volumetric Video Streaming*. Association for Computing Machinery, New York, NY, USA. <https://doi.org/10.1145/3372224.3380888>
- [38] T. Henderson, S. Floyd, A. Gurtov, and Y. Nishida. 2012. The NewReno Modification to TCP's Fast Recovery Algorithm. <https://datatracker.ietf.org/doc/html/rfc6582>.
- [39] A. Horé and D. Ziou. 2010. Image Quality Metrics: PSNR vs. SSIM. In *2010 20th International Conference on Pattern Recognition*. 2366–2369. <https://doi.org/10.1109/ICPR.2010.579>
- [40] Tianchi Huang, Rui-Xiao Zhang, Chao Zhou, and Lifeng Sun. 2018. Qarc: Video quality aware rate control for real-time video streaming based on deep reinforcement learning. In *Proceedings of the 26th ACM international conference on Multimedia*. 1208–1216.
- [41] Junchen Jiang, Vyas Sekar, and Hui Zhang. 2012. Improving fairness, efficiency, and stability in http-based adaptive video streaming with festive. In *Proceedings of the 8th international conference on Emerging networking experiments and technologies*. 97–108.
- [42] Jing Zhu, R. Vannithamby, C. Rödbro, Mingyu Chen, and S. Vang Andersen. 2012. Improving QoE for Skype video call in Mobile Broadband Network. In *2012 IEEE Global Communications Conference (GLOBECOM)*. 1938–1943. <https://doi.org/10.1109/GLOCOM.2012.6503399>
- [43] Hanbyul Joo, Hao Liu, Lei Tan, Lin Gui, Bart Nabbe, Iain Matthews, Takeo Kanade, Shohei Nobuhara, and Yaser Sheikh. 2015. Panoptic Studio: A Massively Multiview System for Social Motion Capture. In *2015 IEEE International Conference on Computer Vision (ICCV)*. <https://doi.org/10.1109/ICCV.2015.381>
- [44] I. Kadota and E. Modiano. 2019. Minimizing the Age of Information in Wireless Networks with Stochastic Arrivals. *IEEE Transactions on Mobile Computing* (2019), 1–1. <https://doi.org/10.1109/TMC.2019.2959774>
- [45] Dina Katabi, Mark Handley, and Charlie Rohrs. 2002. Congestion Control for High Bandwidth-Delay Product Networks. *SIGCOMM Comput. Commun. Rev.* (2002). <https://doi.org/10.1145/964725.633035>
- [46] Sanjit Kaul, Marco Gruteser, Vinuth Rai, and John Kenney. 2011. Minimizing age of information in vehicular networks. In *Proc. IEEE Communications Society Conference on Sensor, Mesh and Ad Hoc Communications and Networks*.
- [47] Eymen Kurdoglu, Yong Liu, Yao Wang, Yongfang Shi, ChenChen Gu, and Jing Lyu. 2016. Real-time bandwidth prediction and rate adaptation for video calls over cellular networks. In *Proceedings of the 7th International Conference on Multimedia Systems*. 1–11.
- [48] Kyungjin Lee, Juheon Yi, Youngki Lee, Sunghyun Choi, and Young Min Kim. 2020. *GROOT: A Real-Time Streaming System of High-Fidelity Volumetric Videos*. Association for Computing Machinery, New York, NY, USA.
- [49] A. Milan, L. Leal-Taixé, I. Reid, S. Roth, and K. Schindler. 2016. MOT16: A Benchmark for Multi-Object Tracking. *arXiv:1603.00831 [cs]* (March 2016). <http://arxiv.org/abs/1603.00831> arXiv: 1603.00831.
- [50] Radhika Mittal, Vinh The Lam, Nandita Dukkkipati, Emily Blem, Hassan Wassel, Monia Ghobadi, Amin Vahdat, Yaogong Wang, David Wetherall, and David Zats. 2015. TIMELY: RTT-Based Congestion Control for the Datacenter. In *Proceedings of the 2015 ACM Conference on Special Interest Group on Data Communication* (London, United Kingdom). Association for Computing Machinery, New York, NY, USA. <https://doi.org/10.1145/2785956.2787510>
- [51] Arvind Narayanan, Eman Ramadan, Jason Carpenter, Qingxu Liu, Yu Liu, Feng Qian, and Zhi-Li Zhang. 2020. A First Look at Commercial 5G Performance on Smartphones. In *Proc. The Web Conference, ACM*.
- [52] Arvind Narayanan, Xumiao Zhang, Ruiyang Zhu, Ahmad Hassan, Shuwei Jin, Xiao Zhu, Xiaoxuan Zhang, Denis Rybkin, Zhengxuan Yang, Zhuoqing Morley Mao, Feng Qian, and Zhi-Li Zhang. 2021. A Variegated Look at 5G in the Wild: Performance, Power, and QoE Implications. In *Proceedings of the 2021 ACM SIGCOMM 2021 Conference*. Association for Computing Machinery, New York, NY, USA.
- [53] Ravi Netravali, Anirudh Sivaraman, Somak Das, Ameesh Goyal, Keith Winstein, James Mickens, and Hari Balakrishnan. 2015. Mahimahi: Accurate Record-and-Replay for HTTP. In *Proc. USENIX ATC*.
- [54] Abhay K. Parekh and Robert G. Gallager. 1993. A Generalized Processor Sharing Approach to Flow Control in Integrated Services Networks: The Single-node Case. *IEEE/ACM Trans. Netw.* (1993).
- [55] Darijo Raca, Dylan Leahy, Cormac J. Sreenan, and Jason J. Quinlan. 2020. Beyond Throughput, the next Generation: A 5G Dataset with Channel and Context Metrics. In *Proceedings of the 11th ACM Multimedia Systems Conference* (Istanbul, Turkey). Association for Computing Machinery, New York, NY, USA.
- [56] Devdeep Ray, Jack Kosaian, K. V. Rashmi, and Srinivasan Seshan. 2019. Vantage: Optimizing Video Upload for Time-Shifted Viewing of Social Live Streams. In *Proceedings of the ACM Special Interest Group on Data Communication* (Beijing, China) (*SIGCOMM '19*). New York, NY, USA.
- [57] S. Blake and D. Black and M. Carlson and E. Davies and Z. Wang and W. Weiss. 1998. An Architecture for Differentiated Services. <https://tools.ietf.org/html/rfc2475>.
- [58] T. Schierl, C. Hellge, S. Mirta, K. Gruneberg, and T. Wiegand. 2007. Using H.264/AVC-based Scalable Video Coding (SVC) for Real Time Streaming in Wireless IP Networks. In *2007 IEEE International Symposium on Circuits and Systems*. 3455–3458. <https://doi.org/10.1109/ISCAS.2007.378370>
- [59] H. Schwarz, D. Marpe, and T. Wiegand. 2007. Overview of the Scalable Video Coding Extension of the H.264/AVC Standard. *IEEE Transactions on Circuits and Systems for Video Technology* 17, 9 (2007), 1103–1120. <https://doi.org/10.1109/TCSVT.2007.905532>
- [60] M. Shreedhar and George Varghese. 1995. Efficient Fair Queueing Using Deficit Round Robin. *ACM SIGCOMM Computer Communication Review* (1995).
- [61] Anirudh Sivaraman, Suvinay Subramanian, Mohammad Alizadeh, Sharad Chole, Shang-Tse Chuang, Anurag Agrawal, Hari Balakrishnan, Tom Edsall, Sachin Katti, and Nick McKeown. 2016. Programmable Packet Scheduling at Line Rate. In *Proceedings of the 2016 ACM SIGCOMM Conference (SIGCOMM '16)*.
- [62] G. J. Sullivan, J. Ohm, W. Han, and T. Wiegand. 2012. Overview of the High Efficiency Video Coding (HEVC) Standard. *IEEE Transactions on Circuits and Systems for Video Technology* (2012).
- [63] Software Radio Systems(SRS). 2021. srsRAN Your own mobile network. <https://www.srsite.com/>.

- [64] Chia-Hui Tai, Jiang Zhu, and Nandita Dukkkipati. 2008. Making Large Scale Deployment of RCP Practical for Real Networks. In *INFOCOM 2008. 27th IEEE International Conference on Computer Communications, Joint Conference of the IEEE Computer and Communications Societies, 13-18 April 2008, Phoenix, AZ, USA*.
- [65] Balajee Vamanan, Jahangir Hasan, and T.N. Vijaykumar. 2012. Deadline-Aware Datacenter Tcp (D2TCP). In *Proceedings of the ACM SIGCOMM 2012 Conference on Applications, Technologies, Architectures, and Protocols for Computer Communication* (Helsinki, Finland). Association for Computing Machinery, New York, NY, USA. <https://doi.org/10.1145/2342356.2342388>
- [66] T. Wiegand, G.J. Sullivan, G. Bjontegaard, and A. Luthra. 2003. Overview of the H.264/AVC video coding standard. *IEEE Transactions on Circuits and Systems for Video Technology* (2003). <https://doi.org/10.1109/TCSVT.2003.815165>
- [67] M. Wien, R. Cazoulat, A. Graffunder, A. Hutter, and P. Amon. 2007. Real-Time System for Adaptive Video Streaming Based on SVC. *IEEE Transactions on Circuits and Systems for Video Technology* 17, 9 (2007), 1227–1237. <https://doi.org/10.1109/TCSVT.2007.905519>
- [68] Christo Wilson, Hitesh Ballani, Thomas Karagiannis, and Ant Rowtron. 2011. Better Never than Late: Meeting Deadlines in Datacenter Networks (*SIGCOMM '11*). Association for Computing Machinery, New York, NY, USA. <https://doi.org/10.1145/2018436.2018443>
- [69] Keith Winstein, Anirudh Sivaraman, and Hari Balakrishnan. 2013. Stochastic Forecasts Achieve High Throughput and Low Delay over Cellular Networks. In *Proc. USENIX NSDI*.
- [70] Yaxiong Xie, Fan Yi, and Kyle Jamieson. 2020. PBE-CC: Congestion Control via Endpoint-Centric, Physical-Layer Bandwidth Measurements. In *Proceedings of the Annual Conference of the ACM Special Interest Group on Data Communication on the Applications, Technologies, Architectures, and Protocols for Computer Communication*. <https://doi.org/10.1145/3387514.3405880>
- [71] Mao Yang, Yong Li, Depeng Jin, Li Su, Shaowu Ma, and Lieguang Zeng. 2013. OpenRAN: A Software-Defined Ran Architecture via Virtualization. In *Proceedings of the ACM SIGCOMM 2013 Computer Communication Review* (Hong Kong, China). Association for Computing Machinery, New York, NY, USA. <https://doi.org/10.1145/2486001.2491732>
- [72] Yasir Zaki, Thomas Pötsch, Jay Chen, Lakshminarayanan Subramanian, and Carmelita Görg. 2015. Adaptive Congestion Control for Unpredictable Cellular Networks. In *Proceedings of the 2015 ACM Conference on Special Interest Group on Data Communication (SIGCOMM '15)*. <https://doi.org/10.1145/2785956.2787498>
- [73] Ben Zhang, Xin Jin, Sylvia Ratnasamy, John Wawrzyniek, and Edward A. Lee. 2018. AWStream: Adaptive Wide-area Streaming Analytics. In *Proceedings of the ACM Special Interest Group on Data Communication (SIGCOMM '18)*.
- [74] Yunfei Zhang, Gang Li, Chunshan Xiong, Yixue Lei, Wei Huang, Yunbo Han, Anwar Walid, Y. Richard Yang, and Zhi-Li Zhang. 2020. MoWIE: Toward Systematic, Adaptive Network Information Exposure as an Enabling Technique for Cloud-Based Applications over 5G and Beyond (Invited Paper) (*NAI '20*). New York, NY, USA. <https://doi.org/10.1145/3405672.3409489>
- [75] Zhou Wang, A. C. Bovik, H. R. Sheikh, and E. P. Simoncelli. 2004. Image quality assessment: from error visibility to structural similarity. *IEEE Transactions on Image Processing* 13, 4 (2004), 600–612. <https://doi.org/10.1109/TIP.2003.819861>
- [76] Yibo Zhu, Haggai Eran, Daniel Firestone, Chuanxiong Guo, Marina Lipshteyn, Yehonatan Liron, Jitendra Padhye, Shachar Raindel, Mohammad Haj Yahia, and Ming Zhang. 2015. Congestion Control for Large-Scale RDMA Deployments. In *Proceedings of the 2015 ACM*

Conference on Special Interest Group on Data Communication (London, United Kingdom). Association for Computing Machinery, New York, NY, USA. <https://doi.org/10.1145/2785956.2787484>

Appendix

A Dropping primitives in P4

As a proof-of-concept to show implementation feasibility of Octopus’s dropping primitives in hardware, we implement Octopus’ dropping primitives in P4[16] bmv2. Octopus maintains a table of latest dropper messages, indexed by the priority threshold. It refers to this table at the egress to determine whether the packet should be dropped or forwarded. This table must be updated when a dropper message arrives at the ingress. However, P4 does not allow sharing memory between ingress and egress. We resolve this issue by cloning the tail packet of the dropper message at the ingress and sending this clone in high priority. This allows the egress to dequeue the clone and update the drop table before dequeuing regular data packets sent at a lower priority. The egress drops the clone after updating the table. Algorithm2 is the pseudocode for the P4 implementation logic.

Algorithm 2 Semantic packet drops in P4

```

procedure INGRESS(packet)
  if packet.hasDropFlag() and packet.isTail() then
    packet.priority()  $\leftarrow$  HIGH_PRIO
    Clone(packet)
  end if
  packet.priority()  $\leftarrow$  LOW_PRIO
  return Enqueue(packet)
end procedure
procedure EGRESS(packet)
  Register reg_droppers[NUM_PRIORITY]
  Register reg_current_drop[1]
  if packet.isClone() then
    threshold  $\leftarrow$  packet.priorityThreshold()
    reg_droppers[threshold]  $\leftarrow$  packet.msgID()
    return Drop(packet)
  end if
  msgid  $\leftarrow$  packet.msgID()
  prio  $\leftarrow$  packet.priority()
  if packet.isHead() then
    drop_msgno  $\leftarrow$  max(reg_droppers[0]...reg_droppers[prio])
    isdrop  $\leftarrow$  ( msgid < drop_msgno
      or packet.bitrate() > dequeueRate() )
    if isdrop then
      reg_current_drop[0]  $\leftarrow$  msgid
    end if
  end if
  if reg_current_drop[0] = msgid then
    return Drop(packet)
  end if
  return Dequeue(packet)
end procedure

```

B Supplementary case study results

We provide several additional case study results in this section. Figure 13 shows the median latency and SQI-SSIM QoE metrics of Octopus and other baselines for real-time video with quality adaptation. All systems achieve similar low median latency, and Octopus has the highest video quality across all systems.

Figure 14 and Figure 15 show the experiment results of the second case study with 120ms RTT. Octopus achieves similar performance improvement than other baselines. Compared with scenarios with 60ms RTT, all systems have lower video quality and slightly higher tail latency due to longer RTT and slower network feedback for congestion control. Figure 16 shows the experiment results of real-time volumetric video streaming with 120ms RTT. Octopus performs better than ViVo in both video quality and tail latency.

C Link Utilization on Legacy switches

Figure 17 shows the link utilizations of OctoBBR and Salsify competing with a backlogged TCP flow on a legacy switch. In this case, OctoBBR earns a fair share of link capacity since its endhost congestion control is BBR. However, Salsify suffers from low link utilization due to its conservative behavior.

D Results with multiple bottlenecks

In Figure 18, we evaluate Octopus and baselines from §6.2, but in a scenario with multiple bottlenecks. The first bottleneck is at a legacy (non-Octopus) switch with a bandwidth of 12Mbps, and the second is a cellular (Octopus) link with bandwidths drawn from the Verizon downlink trace. We see similar performance trends as those in §6.2.

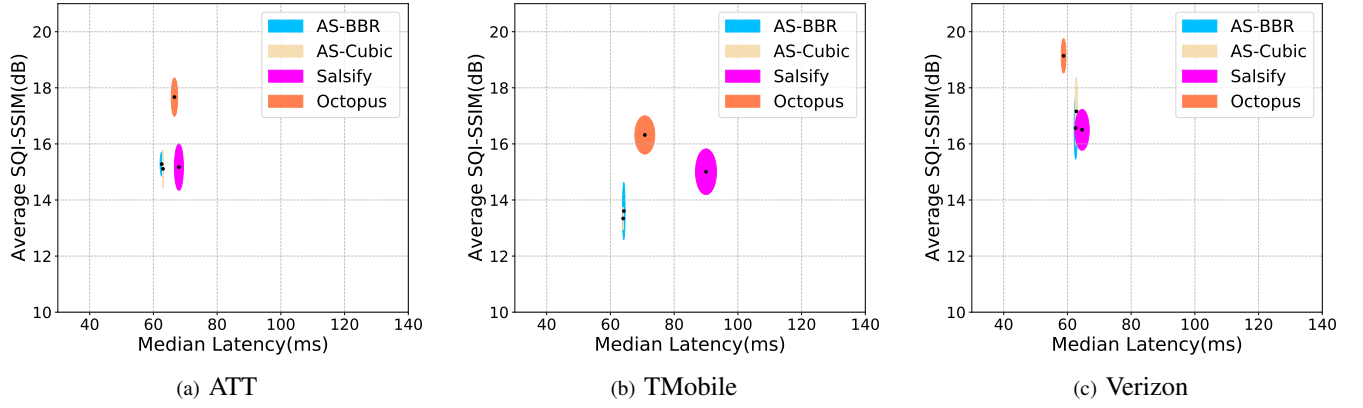


Figure 13: The median latency v.s. video quality of Octopus and other baselines in different LTE download traces with RTT 60ms. The axes of the ellipse reflect the standard deviations in SQI-SSIM and median latency.

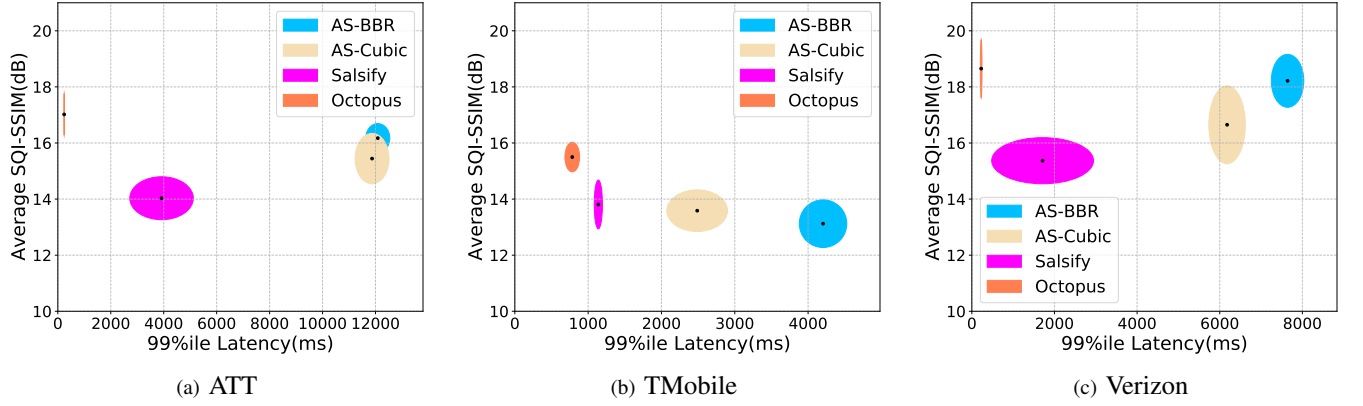


Figure 14: The 99%ile tail latency v.s. video quality of Octopus and other baselines in different LTE download traces with RTT 120ms.

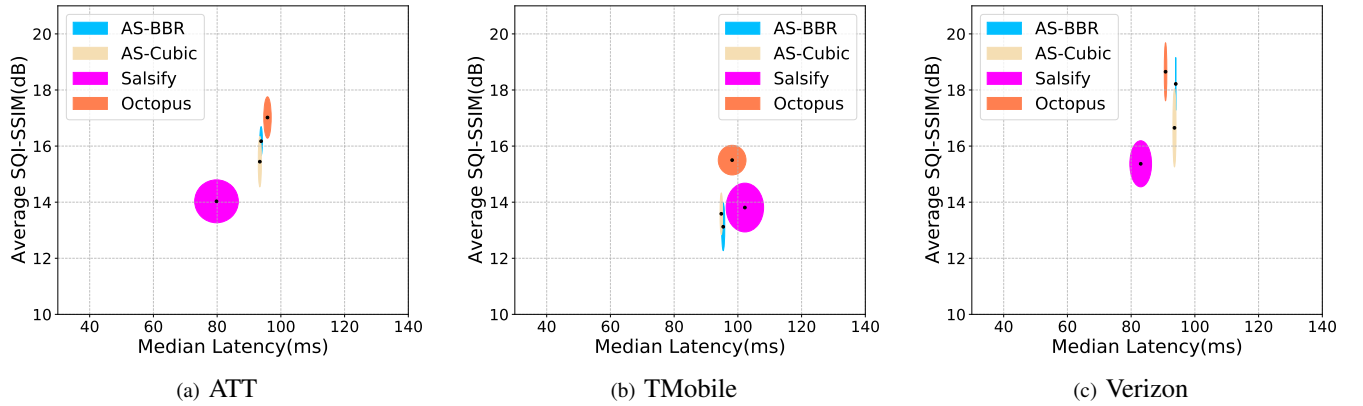


Figure 15: The median latency v.s. video quality of Octopus and other baselines in different LTE download traces with RTT 120ms.

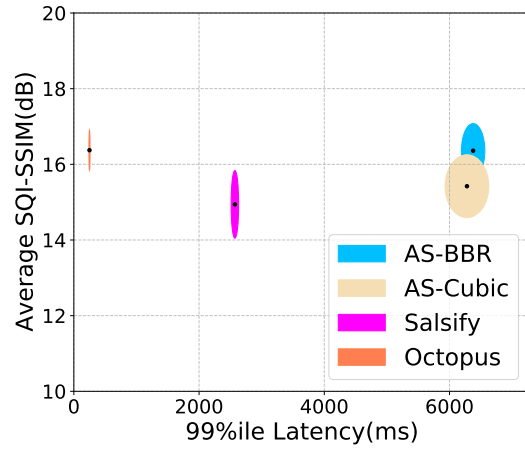


Figure 18: Real-time video with quality adaptation in scenarios with multiple bottlenecks.

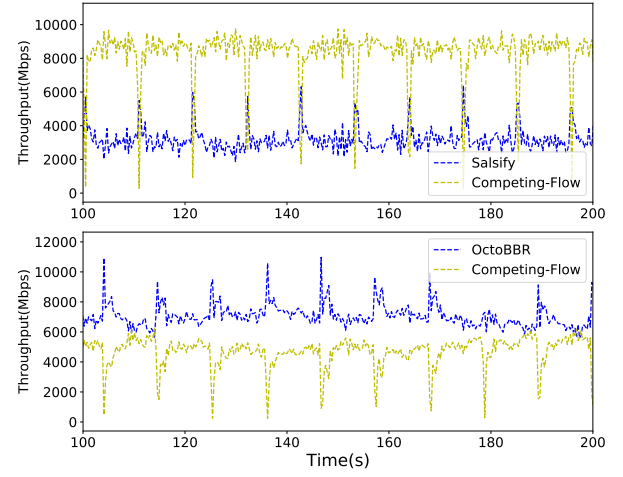


Figure 17: The throughput time series graph of OctoBBR and Salsify sharing the 12Mbps ethernet link with a competing flow.

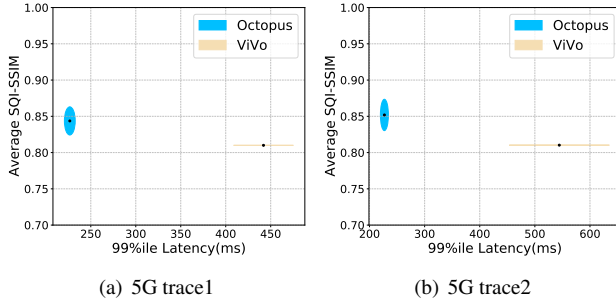


Figure 16: The 99% tail latency v.s. volumetric video quality of Octopus and ViVo in two 5G traces with RTT 120ms.